Revisiting the Observed Correlation Between Weekly Averaged Indian Monsoon Precipitation and Arabian Sea Aerosol Optical Depth

Disha Sharma[1,2] and Ron L. Miller[1]

[1] NASA Goddard Institute for Space Sciences, New York NY

[2] School of Environmental Sciences, Jawaharlal Nehru University, New Delhi, India

Corresponding author: Disha Sharma (disha.sharma@nasa.gov)

Key Points:

- The observed weekly correlation between Indian monsoon rainfall and Arabian Sea dust can be simulated without dust radiative effects.
- The model correlation results from the effect of the monsoon circulation upon dust emission and transport from the Arabian Peninsula.
- The effect of dust radiative heating upon synoptic (few-day) variations of monsoon precipitation remains unknown.

Abstract

Dust influences the Indian summer monsoon on seasonal timescales by perturbing atmospheric radiation. On weekly time scales, aerosol optical depth retrieved by satellite over the Arabian Sea is correlated with Indian monsoon precipitation. This has been interpreted to show the effect of dust radiative heating on Indian rainfall on synoptic (few-day) time scales. However, this correlation is reproduced by Earth System Model simulations, where dust is present but its radiative effect is omitted. Analysis of daily variability suggests that the correlation results from the effect of precipitation on dust through the associated cyclonic circulation. Boundary layer winds that deliver moisture to India are responsible for dust outbreaks in source regions far upwind, including the Arabian Peninsula. This suggests that synoptic variations in monsoon precipitation over India enhance dust emission and transport to the Arabian Sea. The effect of dust radiative heating upon synoptic monsoon variations remains to be determined.

1. Introduction

Airborne soil particles (or mineral dust aerosol) influence the global atmospheric circulation and climate by perturbing Earth's radiative balance through scattering and absorption [*Coakley and Cess,* 1985; *Andrea,* 1995; *Tegen and Lacis,* 1996, *Miller et al.,* 2014]. In addition, dust alters climate indirectly by serving as nucleation sites for cloud water droplets and ice crystals [*Nenes and Murray*, 2014], while supplying iron to ocean ecosystems, catalyzing photosynthesis and drawing down atmospheric CO_2 [*Mahowald et al.,* 2011].

The summer monsoon provides the bulk of precipitation to India, and even small interannual variations can disproportionately impact economies and ecosystems throughout South Asia [*Webster et al.,* 1998; *Gadgil,* 2003]. The role of aerosols in the seasonal and subseasonal modulation of summertime rainfall over India has long been the subject of scientific investigation [*Chung et al.,* 2002; *Menon et al.,* 2002; *Ramanathan et al.,* 2005; *Chung and Ramanathan,* 2006; *Lau et al.,* 2006; *Nigam and Bollasina,* 2010; *Das et al.,* 2015; *Solmon et al.,* 2015, *Kulshrestha and Sharma,* 2015]. Dust is one of the major contributors to the aerosol load over the Indian subcontinent due to long range transport from North Africa and West Asia

(including the Arabian Peninsula), with the Great Indian Thar Desert as a local source [*Prospero et al*. 2002, *Dey et al*., 2004; *Gautam et al*., 2010, *Sharma and Kulshrestha, 2014, Kumar et al., 2015*]. This highlights the role of the atmospheric circulation in aerosol loading from distant sources [*Kaskaoutis et al*., 2014], where phenomena local to the Indian Ocean like tropical cyclones raise dust far upwind [*Ramaswamy,* 2014]. In addition, through dynamical adjustment, the effect of dust upon climate and precipitation can extend thousands of kilometers beyond the region of highest aerosol concentration [*Miller et al*. 2014].

Various mechanisms have been described by which aerosols modify the Indian monsoon. Aerosols generally reduce net radiation into the surface, and this dimming requires a compensating decrease in the energy flux from the surface to the atmosphere, or else energy import by the ocean circulation [*Miller and Tegen,* 1998, *Miller et al*., 2004b, *Ramanathan et al*., 2005, *Strong et al.,* 2015]. The anomalous surface energy flux includes changes to evaporation that supply moisture to the atmosphere. Precipitation is also altered by radiative heating within the dust layer that is compensated at equilibrium by anomalous vertical motion or diabatic heating (including latent heating). Solar absorption within an aerosol layer acts as an elevated heat source, although its relation to anomalous ascent precipitation on seasonal time scales remains under discussion [*Lau et al*., 2006, *Bollasina et al*. 2008, *Nigam and Bollasina,* 2010; *Kuhlmann and Quaas,* 2010, *Wonsick et al*., 2014, *Miller et al*., 2014]. In general, the adjustment to dust radiative heating by perturbations to the energy and water cycles is complicated and occurs over a broader scale than the spatial extent of the aerosol layer [*Miller et al.,* 2014].

Aerosols reduce the transport of moisture from the Indian Ocean to the subcontinent during Northern Hemisphere (NH) summer [*Ramanathan et al*., 2005, *Ganguly et al*., 2012], which these authors attribute to an aerosol weakening of the meridional temperature contrast between land and sea. *Meehl et al*. [2008] invoke the same mechanism to attribute an increase in the model monsoon circulation to carbonaceous aerosols during the pre-monsoon season. *Bollasina et al*. [2011] describe a similar mechanism, where aerosols reduce the energy gain within the ascending branch of the monsoon circulation, reducing meridional overturning and moisture import. Despite the conflicting impact and variety of physical effects by which aerosols influence the monsoon, there is general agreement that aerosols are needed to account for observations of decreasing monsoon

precipitation during recent decades [*Bollasina et al.,* 2011], especially absorbing aerosol species [*Ramanathan et al.,* 2005, *Wang et al.,* 2009].

The sensitivity of the Indian monsoon to aerosol radiative forcing has been studied mostly on interannual to climatological timescales [e.g. *Menon et al.,* 2002; *Ramanathan et al.,* 2005; *Lau et al.,* 2006; *Meehl et al.,* 2008; *Wang et al.,* 2009; *Bollasina et al.,* 2011]. For example, *Solmon et al.* [2015] find that prescribing interannual variations in emission from dust sources over the Arabian Peninsula using retrievals of aerosol optical depth brings a model decadal trend of monsoon precipitation into better agreement with observations. Very few studies assess the relation between aerosol radiative forcing and faster, synoptic-scale variations of the monsoon.

One exception is a study by *Vinoj et al.,* [2014], who demonstrated a correlation between weekly averages of NH summer precipitation over central India from the Global Precipitation Climatology Project (GPCP) and retrievals of aerosol optical depth (AOD) by the Moderate Resolution Imaging Scatterometer (MODIS). A week of high precipitation over central India during the summer monsoon is accompanied by high AOD over the northwestern Arabian Sea (with a reduction of AOD along the coast of the Bay of Bengal). *Vinoj et al.,* [2014] show that the correlation is absent in retrievals of AOD corresponding to the fine-aerosol fraction and thus a consequence of coarse-mode natural aerosols such as dust and sea-salt. Experiments with the NCAR Community Atmosphere Model 5 show that the dominant contribution to coarse-mode AOD in this region is by dust aerosols emitted over the Arabian Peninsula. *Vinoj et al.* [2014] interpret the correlation as evidence that direct radiative forcing by dust aerosols over the Arabian Sea drives variations in precipitation over central India on weekly time scales.

In this article, we revisit the interpretation of this observed correlation between Arabian Sea AOD and Indian monsoon precipitation. Using an Earth system model that reproduces this correlation, we examine the relationship between dust aerosols and monsoon precipitation with higher temporal resolution, using daily model output to examine the processes linking these two physical quantities. Significantly, our model is able to reproduce the observed correlation despite the omission of dust radiative forcing, with dust AOD computed solely as a diagnostic. This leads us to hypothesize that the correlation results from the effect of Indian monsoon precipitation on dust

emission over remote sources within the Arabian Peninsula that contribute to AOD over the Arabian Sea.

2. Model Description and Methods

Ten-year simulations were carried out with the NASA Goddard Institute for Space Studies (GISS) Earth System ModelE2. The model version has been updated since its description by *Schmidt et al*. [2014], and reflects a version available in 2016 that features an improved Madden-Julian Oscillation [*Del Genio et al*., 2012; *Kim et al*., 2012], an important component of subseasonal variability over the Indian Ocean during NH summer [*Zhang and Dong,* 2004]. Model horizontal resolution is 2° latitude by 2.5° longitude with 40 vertical layers. Dust sources correspond to topographic basins where vegetation that binds the soil particles is sparse [*Ginoux et al*., 2001]. Dust emission, transport and deposition are calculated according to *Miller et al*. [2006], except for the addition of a size category for large particles (with radii between 8 and 16 μm), along with an updated wet removal scheme [*Perlwitz et al*. 2015]. Global, annual emission for particles with radii less than 8 μm is 1400 Tg, while the corresponding load is 19 Tg. These values are within the observed range, although on the low end [*Kok et al*., 2017]. Emission increases non-linearly with the surface wind speed that is updated every fifteen minutes in the model, but also increases as a result of intense but ephemeral wind gusts whose effect upon emission is parameterized [*Cakmur et al*., 2004]. The dust aerosol distribution does not modify atmospheric radiation, but aerosol optical depth (AOD) is computed diagnostically, approximating dust particles as Mie scatterers with optical properties taken from the compilation of *Sinyuk et al*. [2003] that includes values retrieved by *Dubovik et al*. [2002] and *Colarco et al*. [2002].

The simulations were carried out with sea surface temperature (SST) prescribed using an observed climatology [*Rayner et al*., 2003]. Use of prescribed SST removes the surface energy balance over the ocean (but not over land), distorting feedbacks between surface radiative forcing by dust, evaporation and the hydrologic cycle [*Miller et al*., 2004b]. However, our interest in this study is the relation between dust and synoptic-scale variations in Indian monsoon precipitation. To a good approximation, SST can be regarded as constant over the lifetime of an individual precipitation event, which is on the order of a week and short compared to the interannual time scale of adjustment for the upper ocean [*Miller,* 2012]. At times longer than a few weeks, adjustment of

the surface energy balance to dust radiative forcing leads to changes in SST and the monsoon [*Miller et al*., 2004b]. However, the dynamics of the synoptic scale variations are assumed to remain approximately unchanged despite the slow adjustment of the surface [c.f. Figure~13 of *Miller,* 2012]. To increase the number of synoptic-scale precipitation events and the statistical significance of their relation to dust, a ten-year simulation is carried out. Model variables are archived every three hours. To exclude the diurnal cycle and emphasize synoptic time scales of a few days, we analyze daily averages, or else values from a single time of day.

To characterize variations of the summer monsoon, we calculate a precipitation index (PI) that is the spatial average of the model precipitation anomaly over grid boxes between 16° to 28° N and 72.5° to 87.5° E. Our choice of area is somewhat arbitrary, but closely resembles that used by previous studies to characterize precipitation over central India [*Gadgil,* 2003, *Goswami et al*., 2006 and *Vinoj et al*., 2014]. This region contains the path of observed synoptic precipitation events [*Gadgil,* 2003]. To emphasize synoptic time scales, we filter periods longer than a month, as described in Text S1 of the supporting information. Figure S1 shows that the high-passed filtered PI is characterized by few-day (synoptic) variations, as observed [*Gadgil,* 2003].

3. Results

3.1. Revisiting the relation between AOD and the Central India Precipitation Index

We first calculate the correlation between weekly averages of dust AOD and the Central India precipitation index (PI). The correlation (Figure 1h) resembles the pattern calculated by *Vinoj et al*. [2014] using MODIS AOD and a precipitation index constructed from GPCP. High rainfall over central India is correlated with enhanced dust AOD over the northwestern Arabian Sea, with reduced AOD over central India and at the head of the Bay of Bengal. (AOD is also reduced over the Arabian Peninsula near the Persian Gulf, within the path of dust delivered to the Arabian Sea from sources within southern Iraq. In Text S3 of the supporting information, we suggest a reason for this negative correlation.)

Vinoj et al. [2014] interprets the positive correlation over the Arabian Sea as evidence that dust in this region is driving variations in rainfall over central India. However, Figure 1h exhibits the same spatial pattern as observed, based upon simulations where dust has no radiative impact and AOD is computed only diagnostically. This suggests that weekly variations of monsoon precipitation over central India do not depend upon the radiative effect of mineral dust, and that some other physical mechanism is responsible for this correlation.

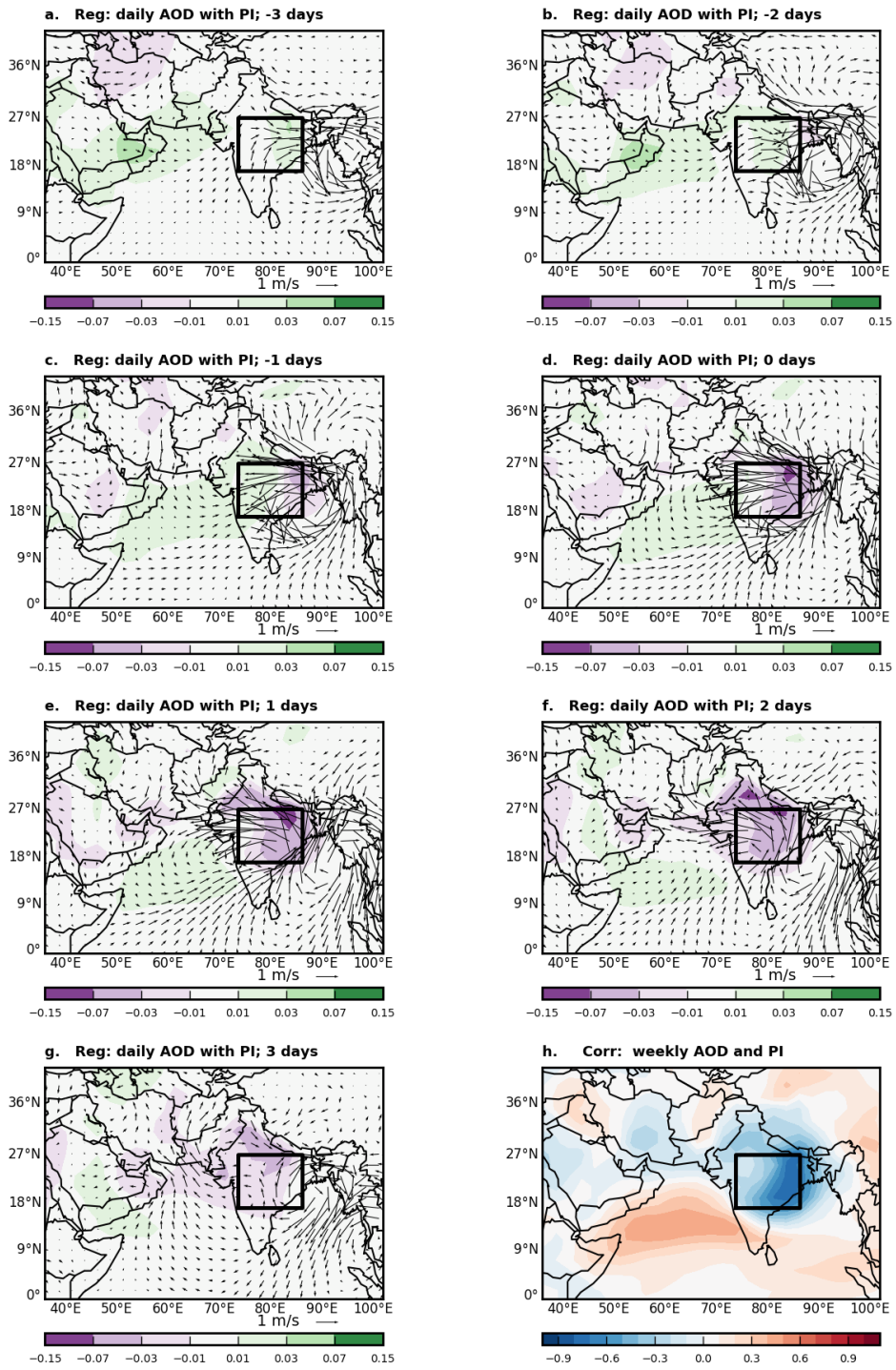

Figure 1. (a-g) Regression of daily-average dust aerosol optical depth (AOD) with the daily normalized Central India Precipitation Index (PI), constructed from precipitation averaged within the rectangle. The regression pattern is dimensionless. The vectors show the regressed model winds near 840 hPa. The lag is relative to the PI; for negative lags, AOD leads precipitation. Panel h: correlation of weekly averages of AOD and the Central India PI following *Vinoj et al*. (2014). Regression and correlation coefficients are calculated for each summer (June 1 through August

31) during the ten-year simulation using the PI normalized separately for each season. The plotted coefficients are an average of the ten summer values.

3.2. Daily variations in precipitation and AOD

To investigate causality between synoptic variations of monsoon precipitation and dust AOD, we examine daily averages of model variables and their relation to the normalized daily PI. (That is, the PI serves as the independent or explanatory variable.) Figure 2 shows the regression of daily precipitation at lags between -3 days (where precipitation leads the PI) and +3 days (where precipitation lags the PI). The regression coefficient is shaded and, due to our normalization of the PI, shows the magnitude of typical synoptic variations of precipitation in mm day^{-1}. Model wind vectors near 840 hPa that are regressed against the PI are also shown. Figure 2 shows the slow westward trajectory of precipitation within a cyclonic vortex. Maximum precipitation over central India (Figure 2d) is preceded by the appearance of the vortex a few days earlier over the eastern Bay of Bengal (Figure 2a). The vortex is trailed by an anticyclonic circulation where precipitation is anomalously low (Figure 2e, f). The vortex pair dissipates a few days after the precipitation maximum over central India, when the seed of a new storm can be seen along the Myanmar coast (Figure 2g). This westward-drifting circulation resembles observed synoptic-scale monsoon depressions described by *Gadgil* [2003] that originate in the Bay of Bengal before traveling over India. The model reproduces the synoptic time scale of the observed events, although the model circulation does not drift as far to the northwest over India as observed (Figure S3). This discrepancy is also evident in the spatial distribution of climatological JJA rainfall shown in Figure S2.

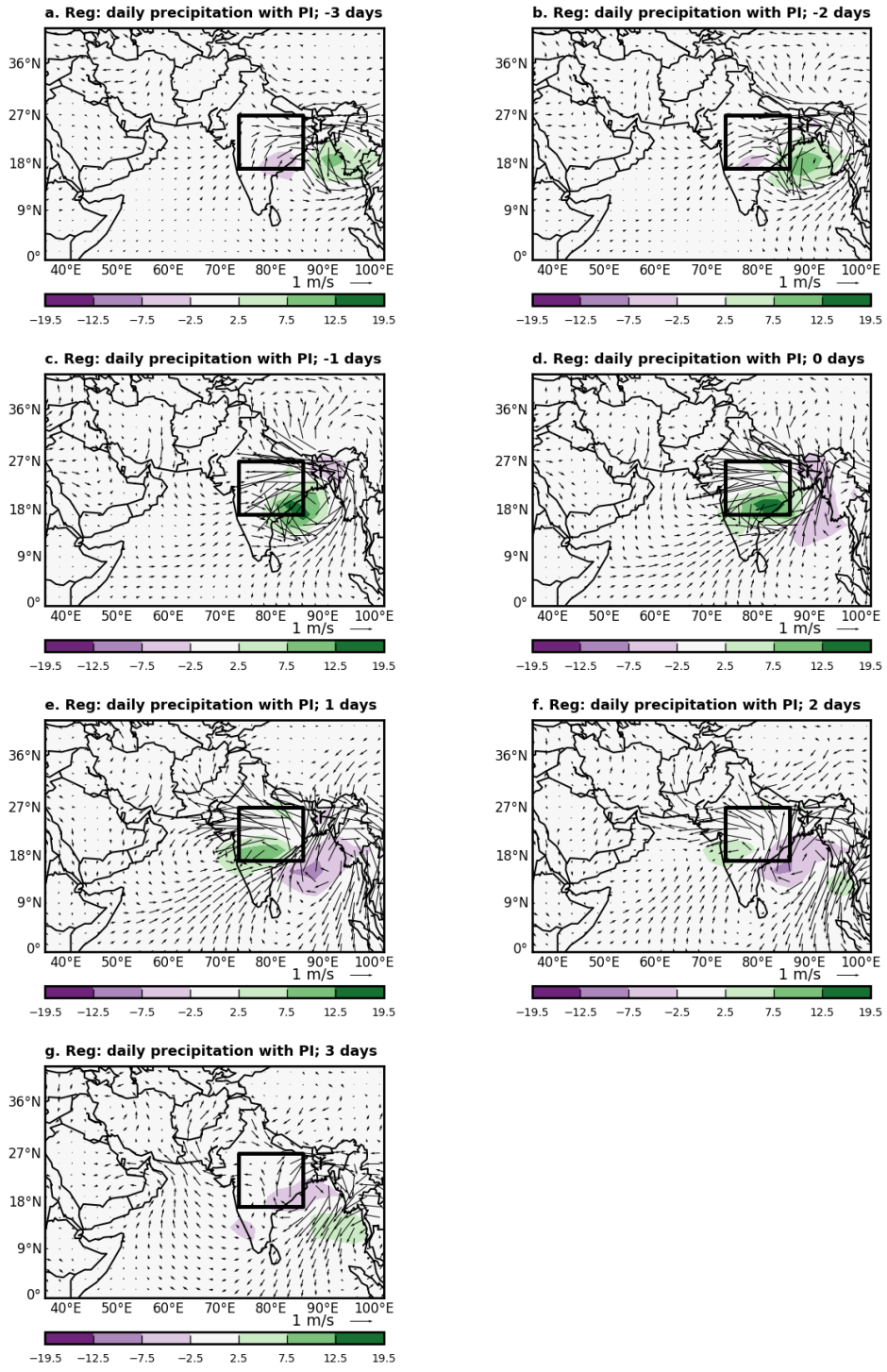

Figure 2. Same as Figure 1 but for daily precipitation in units of mm day^{-1}.

Figure 1 shows the relation between the westward-traveling circulation and AOD. The plume of dust whose weekly averaged AOD is correlated with central India precipitation (Figure 1h) can be

seen to originate over the Arabian Peninsula, drifting to the southeast and crossing the coast at Oman (Figure 1b) as the precipitation moves westward across the Bay of Bengal toward India. This northwesterly flow is part of the low-level regional circulation associated with the precipitation event (as shown by the regressed vector of 840 hPa winds in Figure 1). This synoptic circulation is superimposed on the climatological flow that is northerly or northwesterly over the Arabian Peninsula before turning near the coast to join the monsoon southwesterlies over the Arabian Sea (Figure S2). The dust plume over the Arabian Sea exhibits the highest AOD and is most extensive in the days before the maximum of precipitation over central India, while dispersing in the days following the precipitation maximum. These findings suggest that the correspondence of AOD over the Arabian Sea with central India precipitation, as described by *Vinoj et al*. [2014], is a consequence of dust emission upwind and transport by the low-level circulation associated with westward-drifting synoptic precipitation over the Indian subcontinent.

3.3. Dust emission and surface wind speed associated with the PI

Figure 3 shows dust emission averaged between 0600 and 0900 UTC regressed against the daily averaged PI. Dust emission has a strong diurnal cycle with the greatest mobilization generally between 1000 and 1600 local solar time; the three-hour interval in the figure corresponds to the first half of this period over the Arabian Peninsula, where sources upwind of the Arabian Sea are located. Enhanced emission is apparent along the eastern side of the Arabian Peninsula stretching from southern Iraq and the Tigris-Euphrates plain to the coastal sabkhas bordering the Persian Gulf. These are regions of high and persistent dust concentration indicated by satellite radiances, and identified as dust sources by *Prospero et al*. [2002]. Emission remains anomalously large during most of the lifetime of the vortex (Figures 3).

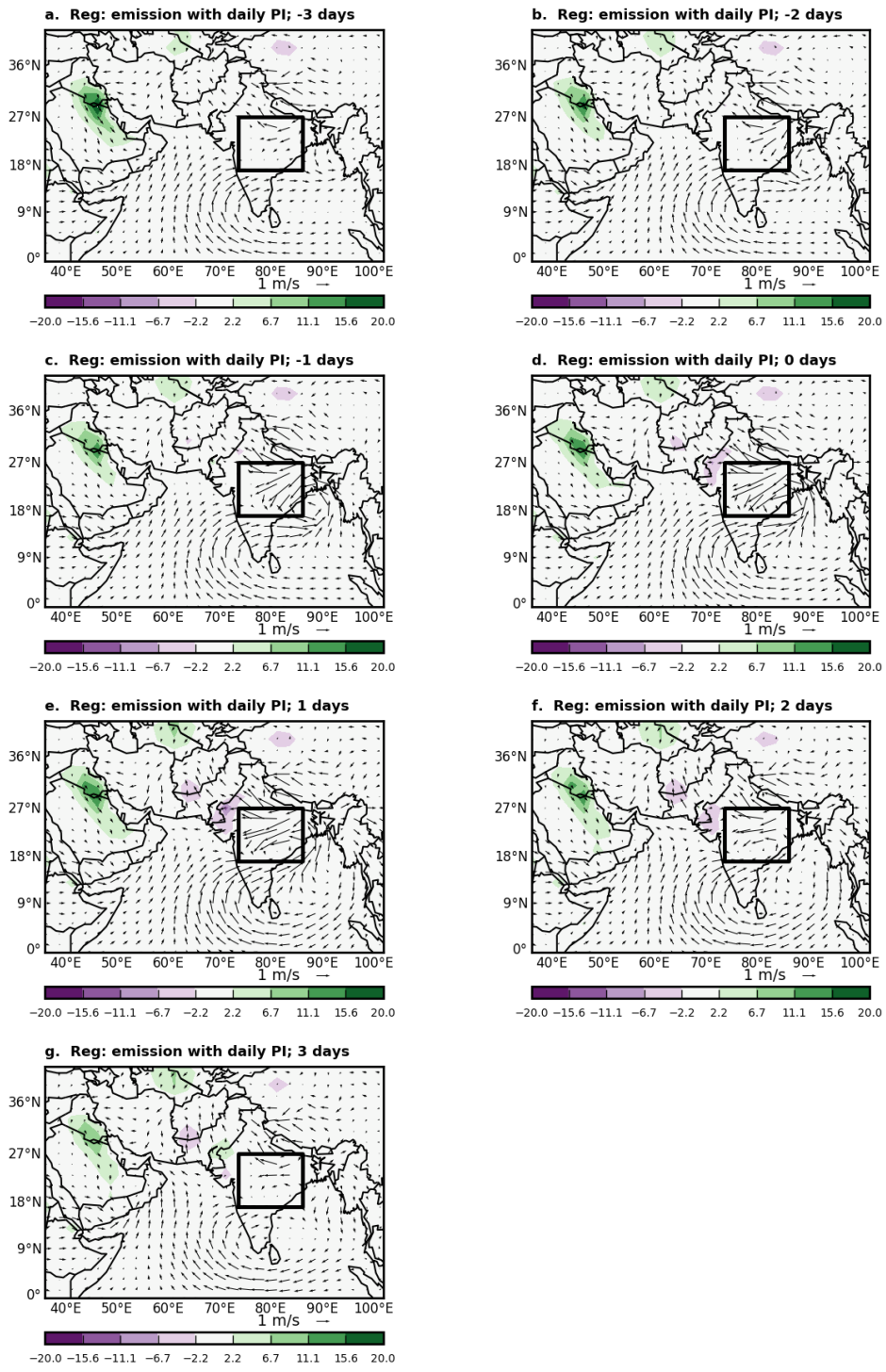

Figure 3. Same as Figure 1 but for dust emission (0600-0900 UTC) in units of μg m^{-2} s^{-1}. Vectors represent the regressed wind in the lowest model layer at the same time of day.

The regression of surface wind speed at the corresponding time (0600-0900 UTC) is shown in Figure 4, with wind vectors corresponding to the lowest model layer. Over dry continental regions, surface wind speed is generally largest in the late morning (local time), after momentum from an overlying nocturnal jet is mixed downward by convective thermals that begin after sunrise [e.g. *Membery,* 1983], consistent with the onset of dust emission around this time [*N'Tchayi Mbourou et al.,* 1997, *Miller et al.,* 2004c, *Allen and Washington,* 2014]. Enhanced dust emission over the Arabian Peninsula (Figure 3) corresponds to where the wind speed anomaly is positive (Figure 4) and reinforces the climatological Shamal winds (Figure S2) that are northerly or northwesterly during this season [*Membery* 1983]. *Notaro et al*. [2013] and *Hamidi et al*. [2013] use station observations and a combination of reanalyses and MODIS images to show that dust emission from this region is often associated with strengthening of the Shamal wind and transport of dust toward the Arabian Sea and monsoon trough, especially during June and July. The wind vectors in Figures 3 and 4 show that reinforcement of the Shamal is part of a larger-scale convergence of the model low-level flow toward the westward-migrating region of low pressure that brings monsoon precipitation to India. *Ramaswamy* [2014] similarly found that tropical cyclones over the Indian Ocean enhance dust emission by strengthening low-level convergence over the Arabian Sea. In contrast, the model synoptic events are more frequent but weaker than the tropical cyclones, with winds around the vortex no stronger than a few meters per second.

The approach of the vortex over central India has an opposite effect upon dust emission over the Thar Desert (Figure 3d-f), where the anomalous cyclonic flow opposes the climatological westerly winds (Figures 4d-f and S2), reducing emission from this source region. Emission is eventually reestablished as the vortex dissipates (Figure 3g).

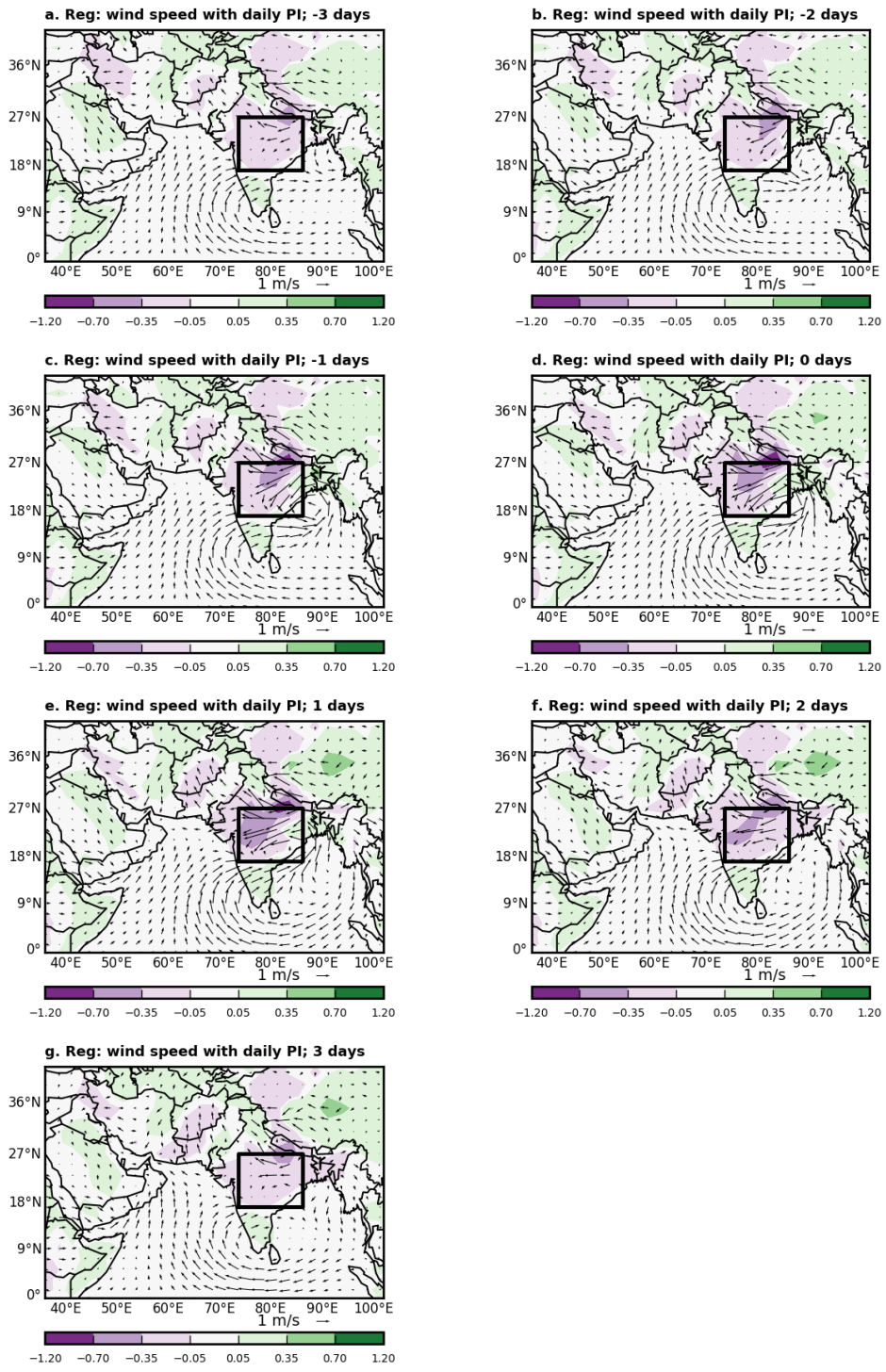

Figure 4. Same as Figure 1 but for wind speed (0600-0900 UTC) in m s^{-1}. To emphasize variations over land, regression coefficients for wind speed are not plotted over the ocean (where they are relatively large). Vectors represent the regressed wind in the lowest model layer at the same time of day.

4. Conclusions

The GISS Earth System ModelE2 reproduces the observed correlation between weekly averages of MODIS aerosol optical depth over the Arabian Sea and Indian monsoon precipitation that was established by *Vinoj et al*. [2014], who showed that dust makes the main contribution among aerosol species to the correlation of AOD, and interpreted this correlation to result from the effect of dust radiative heating upon synoptic variations in monsoon precipitation. However, ModelE2 reproduces this correlation despite omitting the radiative effect of dust. This suggests that radiative heating by dust over the Arabian Sea is not fundamental to variations of monsoon precipitation at weekly and shorter time scales. To identify the physical phenomena responsible for the correlation of dust on monsoon precipitation, we formed a normalized Central India precipitation index that we regressed against daily averaged model output. On synoptic time scales, precipitation over central India is associated with the arrival of a westward-propagating cyclonic circulation (with reduced precipitation within the trailing anticyclone). During the lifetime of this circulation, dust is emitted over the Arabian Peninsula and is transported by the low-level winds to the Arabian Sea. Dust emission is the result of a strengthened Shamal wind along the eastern part of the Arabian Peninsula, including the Tigris-Euphrates basin and the coastal sabkhas of the Persian Gulf. That is, the observed correlation of Arabian Sea AOD and monsoon precipitation is the result of dust emission and transport by the regional circulation associated with the westward-propagating monsoon depressions that bring precipitation to central India.

Other dust sources have been shown to contribute to AOD over the Arabian Sea. For example, *Kaskaoutis et al.* [2014] describe the contribution by the ephemeral drying of marshes within the Sistan Basin near the border of Iran and Afghanistan that are the result of prolonged drought (in that study, attributed to La Niña). The circulation indicated by the regressed wind vectors in Figures 2 and 3 indicates anomalous northerly winds in this region during the lifetime of the Indian monsoon depressions. These northerlies associated with monsoon precipitation correspond to an enhancement of the climatological Levar winds (Figure 4 and S2) that would contribute to Arabian Sea AOD in a model that accounted for these ephemeral sources, or else used a source map giving greater emphasis to this region [e.g. *Ginoux et al.,* 2012].

The impact of dust radiative heating on synoptic precipitation remains unclear. Vinoj et al. (2014) show that the cessation of dust emission leads to a decrease of Indian monsoon precipitation within

ten days. This is interpreted as evidence that dust radiative heating drives variations in monsoon precipitation on this short time scale. However, this evidence is ambiguous since the entire dust load is rapidly eliminated, including both synoptic variations of dust represented by the correlation pattern but also the seasonally varying background distribution of dust upon which the synoptic variations are superimposed. Thus, the initial downward trend of precipitation also includes the fast response to the removal of the background dust [c.f. *Ganguly et al*., 2012], making it impossible to isolate the effect of synoptic scale variations of dust radiative heating and demonstrate a significant impact on precipitation.

On longer (seasonal) time scales, models indicate that dust radiative forcing alters Indian monsoon rainfall [e.g. *Miller et al.,* 2004b, *Solmon et al.,* 2015], although the perturbation depends upon imprecisely known radiative properties of the dust particles [e.g. *Perlwitz and Miller,* 2010, *Jin et al.,* 2016]. On synoptic time scales, the influence of dust upon precipitation remains of unknown magnitude, either as a result of the direct radiative forcing considered here or the effects of dust upon cloud thermodynamics and microphysics. Incorporating radiative effects of dust aerosols has been shown to improve daily forecasts of surface temperature [*Perez et al.,* 2006]. There is a need to better understand the physical processes linking dust radiative heating and precipitation, and the time scales over which this linkage occurs.

Acknowledgments

D. S. was sponsored by a Fulbright Nehru fellowship; we thank the School of Environmental Sciences at Jawaharlal Nehru University for allowing her to pursue research at NASA GISS. Support for R. L. M. was provided by NASA Grant NNG14HH42I from the Modeling, Analysis and Prediction Program. Simulations with the GISS Earth System ModelE2 were made possible by the NASA High-End Computing (HEC) Program through the NASA Center for Climate Simulation (NCCS) at Goddard Space Flight Center. NCEP Reanalysis winds and GPCP precipitation were provided by the Physical Science Division of the NOAA Earth Science Research Laboratory via http://www.esrl.noaa.gov/psd. TRMM Level 3 daily retrievals were provided by the NASA Goddard Earth Sciences Data and Information Services Center via https://disc.gsfc.nasa.gov/datacollection/TRMM_3B42_Daily_7.html. We are grateful for advice by Antara Banerjee, Paul Ginoux, Dr. U. C. Kulshrestha, Carlos Pérez García-Pando, Jan Perlwitz and Dan Westervelt. The manuscript was improved by the thoughtful comments of Richard Washington and an anonymous reviewer.

References:

Allen, C. J. T., and R. Washington (2014), The low-level jet dust emission mechanism in the central Sahara: Observations from Bordj-Badji Mokhtar during the June 2011 Fennec Intensive Observation Period, *J. Geophys. Res. Atmos.,* 119, 2990–3015, doi:10.1002/ 2013JD020594.

Andreae, M. O. (1995), Climatic effects of changing atmospheric aerosol levels, in World Survey of Climatology, vol. 16, Future Climates of the World: A Modelling Perspective, edited by A. Henderson-Sellers, pp. 347–398, Elsevier, New York.

Bollasina, M., S. Nigam, and K.-M. Lau (2008), Absorbing aerosols and summer monsoon evolution over South Asia: An observational portrayal, *J. Climate,* 21, 3221–3239.

Bollasina, M., Ming, Y. & Ramaswamy, V. (2011), Anthropogenic aerosols and the weakening of the South Asian summer monsoon. *Science* 334**,** 502–505.

Cakmur, R. V., R. L. Miller, and O. Torres (2004), Incorporating the effect of small-scale circulations upon dust emission in an atmospheric general circulation model, *J. Geophys. Res.,* 109, D07201, doi:10.1029/2003JD004067.

Chung, C. E., and V. Ramanathan (2006), Weakening of North Indian SST gradients and the monsoon rainfall in India and the Sahel, *J. Clim.,* 19, 2036–2045.

Chung, C. E., V. Ramanathan, and J. T. Kiehl (2002), Effects of the South Asian absorbing haze on the northeast monsoon and surface-air exchange, *J. Clim.,* 15, 2462–2476.

Coakley, J. A., and R. D. Cess (1985), Response of the NCAR Community Climate Model to the radiative forcing by the naturally occurring tropospheric aerosol, *J. Atmos. Sci.,* 42, 1677–1692.

Colarco PR, Toon OB, Torres O, Rasch PJ (2002), Determining the UV imaginary index of refraction of Saharan dust particles from total ozone mapping spectrometer data using a three-dimensional model of dust transport. *J. Geophys. Res.*, 107(D16):4312. doi:10.1029/ 2001JD000903

Das, S., S. Dey, S.K. Dash, G. Guiliani, and F. Solmon (2015), Dust aerosol feedback on Indian

summer monsoon: Sensitivity to absorption property, *J. Geophys. Res. Atmos.,* 120, 9642-9652.

Del Genio, A.D., Y.-H. Chen, D. Kim, and M.-S. Yao (2012), The MJO transition from shallow to deep convection in CloudSat/CALIPSO data and GISS GCM simulations, *J. Climate*, 25, 3755-3770, doi:10.1175/JCLI-D-11-00384.1.

Dey, S., S. N. Tripathi, R. P. Singh, and B. N. Holben (2004), Influence of dust storms on the aerosol optical properties over the Indo-Gangetic Basin, *J. Geophys. Res.,* 109, D20211, doi:10.1029/2004JD004924.

Dubovik O, Holben BN, Eck TF, Smirnov A, Kaufman YJ, King MD, Tanré D, Slutsker I (2002), Variability of absorption and optical properties of key aerosol types observed in worldwide locations, *J. Atmos. Sci.*, 59:590–608.

Gadgil, S. (2003), The Indian monsoon and its variability, *Annu. Rev. Earth Planet. Sci.* , 31**,** 429–467.

Ganguly, D., P. J. Rasch, H. Wang, and J. Yoon (2012), Fast and slow responses of the South Asian monsoon system to anthropogenic aerosols, *Geophys. Res. Lett.,* 39, L18804, doi:10.1029/2012GL053043.

Gautam, R., N. Christina Hsu, and K. M. Lau (2010), Premonsoon aerosol characteristics and radiative effects over the Indo-Gangetic Plains: Implications for regional climate warming, *J. Geophys. Res.,* 115, D17208, doi:10.1029/2010JD013819.

Ginoux, P., M. Chin, I. Tegen, J. Prospero, B. Holben, O. Dubovik, and S. J. Lin (2001), Sources and distributions of aerosols simulated with the GOCART model, *J. Geophys. Res.,* 106, 20,255–20,273.

Goswami, B. N., V. Venugopal, D. Sengupta, M. S. Madhusoodanan, and P. K. Xavier (2006), Increasing trend of extreme rain events over India in a warming environment, *Science,* 314(5804), 1442–1445, doi:10.1126/science.1132027.

Hamidi, M., M. R. Kavianpour, and Y. Shao (2013), Synoptic analysis of dust storms in

the Middle East, *Asia-Pacific Journal of Atmospheric Sciences,* 49(3), 279–286, doi:10.1007/s13143-013-0027-9.

Huffman, G. J., R. F. Adler, D. T. Bolvin, and G. Gu (2009): Improving the global precipitation record: GPCP Version 2.1, *Geophys. Res. Lett.,* 36, L17808, doi:10.1029/2009GL040000.

Huffman, G. J., R. F. Adler, D. T. Bolvin, E. J. Nelkin, 2010: The TRMM Multi-satellite Precipitation Analysis (TMPA). Chapter 1 in Satellite Rainfall Applications for Surface Hydrology, F. Hossain and M. Gebremichael, Eds. Springer Verlag, ISBN: 978-90-481-2914-0, 3-22.

Jin, Q., Yang, Z.-L. and J. Wei (2016), High sensitivity of Indian summer monsoon to Middle East dust absorptive properties, *Scientific Reports* ***6****,* Article number: 30690 doi:10.1038/srep30690.

Kaskaoutis, D., Rashki, A., Houssos, E., Goto, D., and Nastos, P. (2014), Extremely high aerosol loading over Arabian Sea during June 2008: The specific role of the atmospheric dynamics and Sistan dust storms, *Atmos. Environ.,* 94, 374–384.

Kim, D., A.H. Sobel, A. Del Genio, Y.-H. Chen, S.J. Camargo, M.-S. Yao, M. Kelley, and L. Nazarenko (2012), The tropical subseasonal variability simulated in the NASA GISS general circulation model, *J. Climate,* 25, 4641-4659, doi:10.1175/JCLI-D-11-00447.1.

Kok, J. F., D. A. Ridley, Q. Zhou, R. L. Miller, C. Zhao, C. L. Heald, D. S. Ward, S. Albani, and K. Haustein (2017), Smaller desert dust cooling effect estimated from analysis of dust size and abundance. *Nature Geosci*., 10, 274-278, doi:10.1038/ngeo2912.

Kuhlmann, J., and J. Quaas (2010), How can aerosols affect the Asian summer mon- soon? assessment during three consecutive pre-monsoon seasons from CALIPSO satellite data, *Atmos. Chem. Phys.,* 10(10), 4673–4688, doi:10.5194/acp-10-4673- 2010.

Kulshrestha U. C. and D. Sharma, (2015) Importance of atmospheric dust in air: Future scope of research. *Journal of Indian Geophysical Union,* 19, 205-209.

Kumar, B., S. Singh, G. P. Gupta, F. A. Lone and U. C. Kulshrestha (2016), Long Range Transport and Wet Deposition Fluxes of Major Chemical Species in Snow at Gulmarg in North Western Himalayas (India). Aerosol and Air Quality Research, 16, 606–617, 2016, doi: 10.4209/aaqr.2015.01.0056

Lau, K. M., Kim, M. K. & Kim, K. M. (2006), Asian summermonsoon anomalies induced by aerosol direct forcing: The role of the Tibetan Plateau, *Clim. Dynam.*, 26**,** 855–864.

Mahowald, N., D. Ward, S. Kloster, M. Flanner, C. Heald, N. Heavens, P. Hess, J.-F. Lamarque, P. Chuang (2011), Aerosol impacts on climate and biogeochemistry, Annual Reviews of Environment and Resources, 36, 45-74, doi:10.1146/annurev-environ-042009-094507.

Meehl, G. A., Arblaster, J. M. & Collins, W. D. (2008), Effects of black carbon aerosols on the Indian Monsoon, *J. Clim.* , 21**,** 2869–2882.

Membery, D. A. (1983), Low level wind profiles during the Gulf Shamal, *Weather,* 38(1), 18–24, doi:10.1002/j.1477-8696.1983.tb03638.x.

Menon, S., Hansen, J., Nazarenko, L. & Luo, Y. (2002), Climate effects of black carbon aerosols in China and India, *Science* 297**,** 2250–2253.

Miller, R. L., and I. Tegen (1998), Climate response to soil dust aerosols, J. Climate, 11, 3247–3267.

Miller, R. L., I. Tegen, and J. Perlwitz (2004a), Surface radiative forcing by soil dust aerosols and the hydrologic cycle, *J. Geophys. Res.,* 109, D04203, doi:10.1029/2003JD004085.

Miller, R.L., J.P. Perlwitz, and I. Tegen (2004b), Modeling Arabian dust mobilization during the Asian summer monsoon: The effect of prescribed versus calculated SST, *Geophys. Res. Lett.,* 30, L22214, doi:10.1029/2004GL020669.

Miller, R.L., J.P. Perlwitz, and I. Tegen (2004c), Feedback upon dust emission by dust radiative forcing through the planetary boundary layer, *J. Geophys. Res.*, 109, D24209, doi:10.1029/2004JD004912.

Miller, R.L., R.V. Cakmur, J.P. Perlwitz, I.V. Geogdzhayev, P. Ginoux, K.E. Kohfeld, D. Koch, C. Prigent, R. Ruedy, G.A. Schmidt, and I. Tegen (2006), Mineral dust aerosols in the NASA Goddard Institute for Space Sciences ModelE atmospheric general circulation model, *J. Geophys. Res.,* 111, D06208, doi:10.1029/2005JD005796.

Miller, R.L. (2012), Adjustment to radiative forcing in a simple coupled ocean-atmosphere model, *J. Climate*, 25, 7802-7821, doi:10.1175/JCLI-D-11-00119.1.

Miller, R.L., P. Knippertz, C. Pérez García-Pando, J.P. Perlwitz, and I. Tegen (2014), Impact of dust radiative forcing upon climate In *Mineral Dust: A Key Player in the Earth System*. P. Knippertz, and J.-B.W. Stuut, Eds. Springer, 327-357, doi:10.1007/978-94-017-8978-3_13.

N'Tchayi Mbourou, G., J. Bertrand, and S. Nicholson (1997), The diurnal and seasonal cycles of wind-borne dust over Africa north of the equator, *J. Appl. Meteorol.,* 36, 868–882.

Nigam, S., and M. Bollasina (2010), "Elevated heat pump" hypothesis for the aerosol-monsoon hydroclimate link: "Grounded" in observations?, *J. Geophys. Res.*, 115, D16201, doi:10.1029/2009JD013800.

Notaro, M., F. Alkolibi, E. Fadda, and F. Bakhrjy (2013), Trajectory analysis of Saudi Arabian dust storms, *J. Geophys. Res.,* 118(12), 6028–6043, doi: 10.1002/jgrd.50346.

Pérez, C., S. Nickovic, G. Pejanovic, J. M. Baldasano, and E. Özsoy (2006), Interactive dust-radiation modeling: A step to improve weather forecasts, *J. Geophys. Res.,* 111, D16206, doi:10.1029/2005JD006717.

Perlwitz, J., I. Tegen, and R. L. Miller (2001), Interactive soil dust aerosol model in the GISS GCM: 1. Sensitivity of the soil dust cycle to radiative properties of soil dust aerosols, *J. Geophys. Res.,* 106, 18,167–18,192.

Perlwitz, J.P., C. Pérez García-Pando, and R.L. Miller (2015), Predicting the mineral composition of dust aerosols — Part 1: Representing key processes, *Atmos. Chem. Phys.,* 15, 11593-11627, doi:10.5194/acp-15-11593-2015.

Prospero, J. M., P. Ginoux, O. Torres, and S. Nicholson (2002), Environmental characterization of global sources of atmospheric soil dust derived from NIMBUS-7 TOMS absorbing aerosol product, *Rev. Geophys.,* 40, doi:10.1029/2000RG000095.

Ramanathan, V. *et al.,* (2005), Inaugural Article: Atmospheric brown clouds: Impacts on South Asian climate and hydrological cycle, *Proc. Natl Acad. Sci. USA* 102, 5326–5333.

Ramaswamy, V. (2014), Influence of Tropical Storms in the Northern Indian Ocean on Dust Entrainment and Long–Range Transport, in: Typhoon Impact and Crisis Management, 149–174.

Rayner, N. A., Parker, D. E., Horton, E. B., Folland, C. K., Alexander, L. V., Rowell, D. P., Kent, E. C., and Kaplan, A.: Global analyses of sea surface temperature, sea ice, and night marine air temperature since the late nineteenth century, *J. Geophys. Res.,* 108, 4407, doi:10.1029/2002JD002670, 2003.

Schmidt, G.A., M. Kelley, L. Nazarenko, R. Ruedy, G.L. Russell, I. Aleinov, M. Bauer, S.E. Bauer, M.K. Bhat, R. Bleck, V. Canuto, Y.-H. Chen, Y. Cheng, T.L. Clune, A. Del Genio, R. de Fainchtein, G. Faluvegi, J.E. Hansen, R.J. Healy, N.Y. Kiang, D. Koch, A.A. Lacis, A.N. LeGrande, J. Lerner, K.K. Lo, E.E. Matthews, S. Menon, R.L. Miller, V. Oinas, A.O. Oloso, J.P. Perlwitz, M.J. Puma, W.M. Putman, D. Rind, A. Romanou, M. Sato, D.T. Shindell, S. Sun, R.A. Syed, N. Tausnev, K. Tsigaridis, N. Unger, A. Voulgarakis, M.-S. Yao, and J. Zhang (2014), Configuration and assessment of the GISS ModelE2 contributions to the CMIP5 archive, *J. Adv. Model. Earth Syst.,* 6, no. 1, 141-184, doi:10.1002/2013MS000265.

Sharma, D., U.C., Kulshrestha (2014) Spatial and temporal patterns of air pollutants in rural and urban areas of India. *Environmental Pollution,* 195, 276-281, doi:10.1016/j.envpol.2014.08.026.

Sinyuk A, Torres O., Dubovik O. (2003), Combined use of satellite and surface observations to infer the imaginary part of the refractive index of Saharan dust, *Geophys. Res. Lett.*, 30. doi:10.1029/ 2002GL016189.

Solmon, F., V.S. Nair, and M. Mallet (2015), Increasing Arabian dust activity and the Indian summer monsoon, *Atmos. Chem. and Phy.,* 15, 8051-8064.

Strong, J. D., G. A. Vecchi, and P. Ginoux (2015), The response of the tropical Atlantic and West African climate to Saharan dust in a fully coupled GCM, *J. Climate*, doi:10.1175/JCLI- D-14-00797.1.

Tegen, I., and A. A. Lacis (1996), Modeling of particle influence on the radiative properties of mineral dust aerosol, *J. Geophys. Res.,* 101, 19,237–19,244.

Vinoj, V., P. J. Rasch, H. Wang, J. H. Yoon, P. L. Ma, K. Landu, and B. Singh (2014), Short-term modulation of Indian summer monsoon rainfall by West Asian dust, *Nat. Geosci.,* 7(4), 308–313, doi:10.1038/ngeo2107.

Wang, C., Kim, D., Ekman, A. M. L., Barth, M. C. & Rasch, P. J. (2009), Impact of anthropogenic aerosols on Indian summer monsoon, *Geophys. Res. Lett.,* 36, L21704.

Webster, P. J. *et al.,* (1998), Monsoons: Processes, predictability, and the prospects for prediction. *J. Geophys. Res.,* 103**,** 14451–14510.

Wonsick, M. M., R. T. Pinker, and Y. Ma (2014), Investigation of the "elevated heat pump" hypothesis of the Asian monsoon using satellite observations, *Atmos. Chem. Phys.,* 14, 8749–8761, doi:10.5194/acp-14-8749-2014.

Zhang, C., and M. Dong (2004), Seasonality in the Madden–Julian oscillation. *J. Climate*, 17, 3169–3180, doi:10.1175/1520-0442(2004)017<3169:SITMO>2.0.CO;2.

Geophysical Research Letters

Supporting Information for

Revisiting the Observed Correlation Between Weekly Averaged Indian Monsoon Precipitation and Arabian Sea Aerosol Optical Depth

Disha Sharma[1,2] and Ron L. Miller[1]

[1] NASA Goddard Institute for Space Sciences, New York NY

[2] School of Environmental Sciences, Jawaharlal Nehru University, New Delhi, India

Contents of this file

Text S1. Anomaly calculation

Synoptic-scale anomalies of daily averaged variables are calculated by applying a high-pass Blackman filter with a cut-off frequency of 30 days. The filter is applied in the time domain using a moving window with 61 terms, a value chosen to give a sharp reduction in power across the cut-off frequency. As an example, the decomposition of the Central India Precipitation Index

during the first year of the simulation is shown in Figure S1a, where the anomalous (high-frequency) component is in blue, the low-frequency background is in red, and the total is in black. The anomaly is characterized by synoptic-scale (few day) fluctuations in precipitation that are present mainly during NH summer.

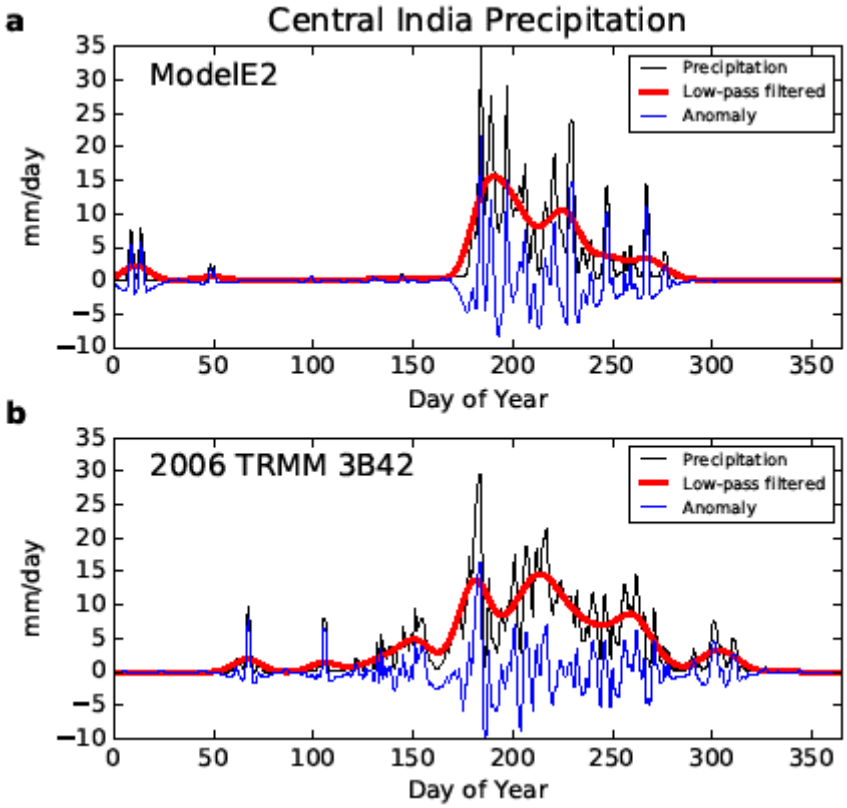

Figure S1. Decomposition of the Central India Precipitation Index a) as simulated by the model during its first year and b) as retrieved by the Tropical Rainfall Measuring Mission (TRMM) during 2006. The anomalous (high-frequency) component is in blue, the low-frequency background is in red, and the total is in black.

Text S2. Representation of the Indian Monsoon in ModelE2

Figure S2 compares the low-level winds and precipitation in the vicinity of the Indian monsoon for NH summer (JJA) as calculated by the NASA GISS Earth System ModelE2 with the National Center for Environmental Prediction (NCEP-NCAR) reanalysis winds [*Kalnay et al.*, 1996] and the Global Precipitation Climatology Project (GPCP) precipitation [*Huffman et al.*, 2009].

The model generally reproduces the magnitude and orientation of the observed circulation, including the cross-equatorial southwesterly flow over the Arabian Sea along with the weaker northwesterly Shamal and northerly Levar winds over the Arabian Peninsula and eastern Iran, respectively, that merge offshore with the southwesterlies. (Neither ModelE2 nor the reanalysis model have sufficient resolution to represent the intricate topography in some regions, complicating the comparison.) Over the Bay of Bengal, the model westerlies are too strong.

The spatial distribution of model precipitation is generally in agreement with the GPCP pattern, although the magnitude of precipitation is excessive in the model, especially along the Myanmar coast and in the foothills of Nepal and Bhutan at the head of the Bay of Bengal. The excessive precipitation in this region is associated with the overestimated cyclonic flow and westerlies across the Bay of Bengal.

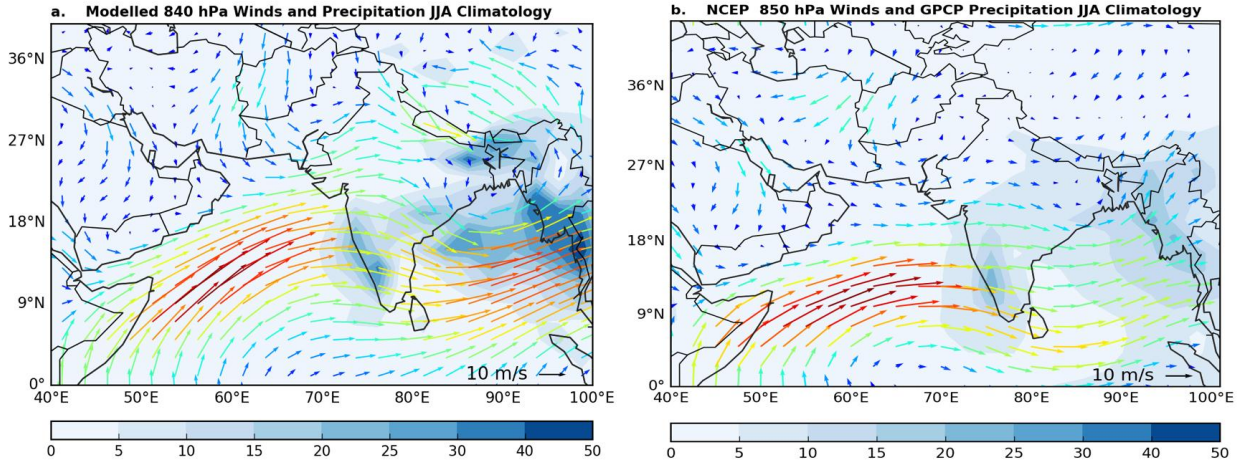

Figure S2. Climatological mean JJA (a) Earth System ModelE2 winds near 840 hPa (ms^{-1}) and precipitation (mm day^{-1}) and (b) NCEP-NCAR 850 hPa winds and GPCP precipitation. The model winds correspond to the seventh sigma-layer in the model, whose height varies with topography and variations of surface pressure. Globally, this level corresponds to an average pressure of 842 hPa.

Precipitation during the summer monsoon is generally observed as traveling depressions that originate over the Bay of Bengal before propagating westward onto the subcontinent [*Gadgil,* 2003]. Figure S3 shows the zonal propagation of daily precipitation, averaged over the latitude band of the Central India Precipitation Index, according to ModelE2 and daily retrievals from the Tropical Rainfall Measuring Mission (TRMM). The latter are derived by merging multi-platform measurements of outgoing longwave radiation along with microwave and radar (Product 3B42, Level 3, Version 7; *Huffman et al.,* 2010). Model simulations use annually

repeating, climatological sea surface temperature, so only general features of the calculated precipitation like the magnitude and frequency of events or the rate of westward displacement can be compared to retrievals that correspond to a particular year. For the sake of illustration, Figure S3 compares ModelE2 to TRMM retrievals from 2006.

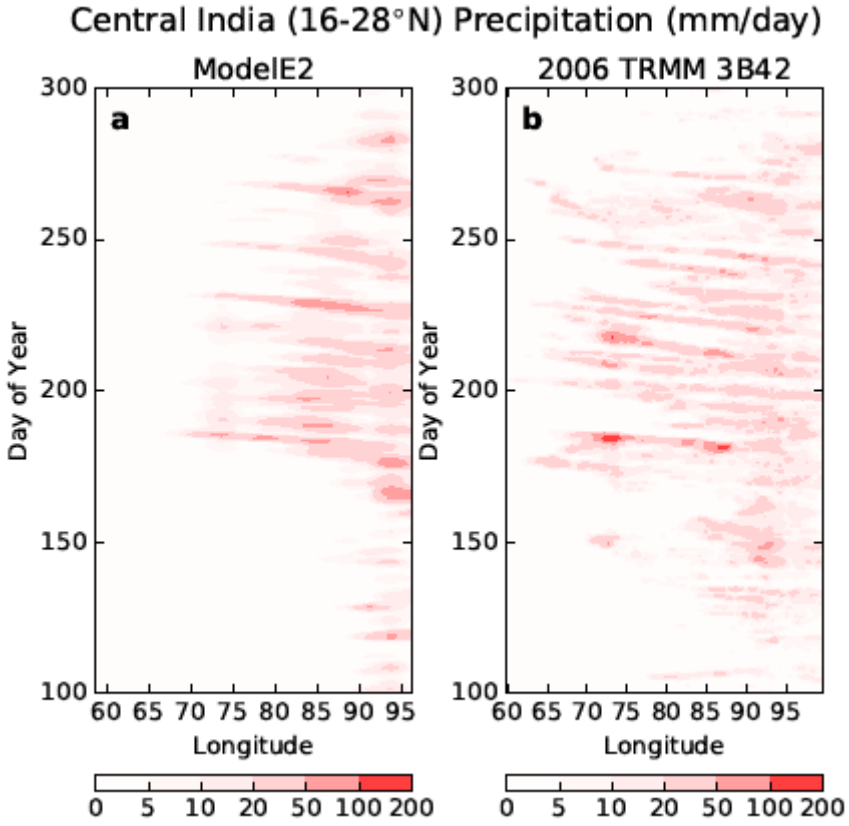

Figure S3. Precipitation (mm day^{-1}) averaged between the latitudes of 16 and 28°N (a) as simulated by ModelE2 during the first year and (b) retrieved by TRMM during 2006.

Monsoon depressions in the model reproduce the general characteristics of precipitation retrieved by TRMM, with onshore propagation from the Bay of Bengal as described by *Gadgil* [2003]. The model depressions show a similar seasonality and move westward at the observed rate, although with a slightly greater zonal extent than observed, presumably an indication that the depressions are only barely resolved by the 2.5° longitudinal spacing of the model grid. Figure S1 similarly shows that synoptic variations of ModelE2 precipitation have a magnitude and frequency over central India that is comparable to those in the TRMM retrievals.

Figure S3 suggests that model depressions dissipate too rapidly as they come onshore, underestimating the delivery of precipitation to the interior of the subcontinent (approximately

west of 80°E). This is corroborated by the spatial distribution of seasonal JJA precipitation in Figure S2, where GPCP precipitation extends to the northwest of India to a greater extent than in the model.

The meridional extent of Indian monsoon precipitation is shown in Figure S4. TRMM retrievals show the largest precipitation centered between 15 and 20°N, with an intermittent secondary maximum south of the equator that is generally associated with monsoon 'breaks' or reduced precipitation over India [*Gadgil,* 2003]. ModelE2 centers its Indian precipitation at the correct latitude, while slightly underestimating the secondary maximum near the equator. The model calculates a spurious secondary maximum of precipitation at the head of the Bay of Bengal and the foothills of the Himalayas. In both the model and TRMM retrievals, some of the traveling monsoon depressions are preceded by the arrival of events propagating from lower latitudes.

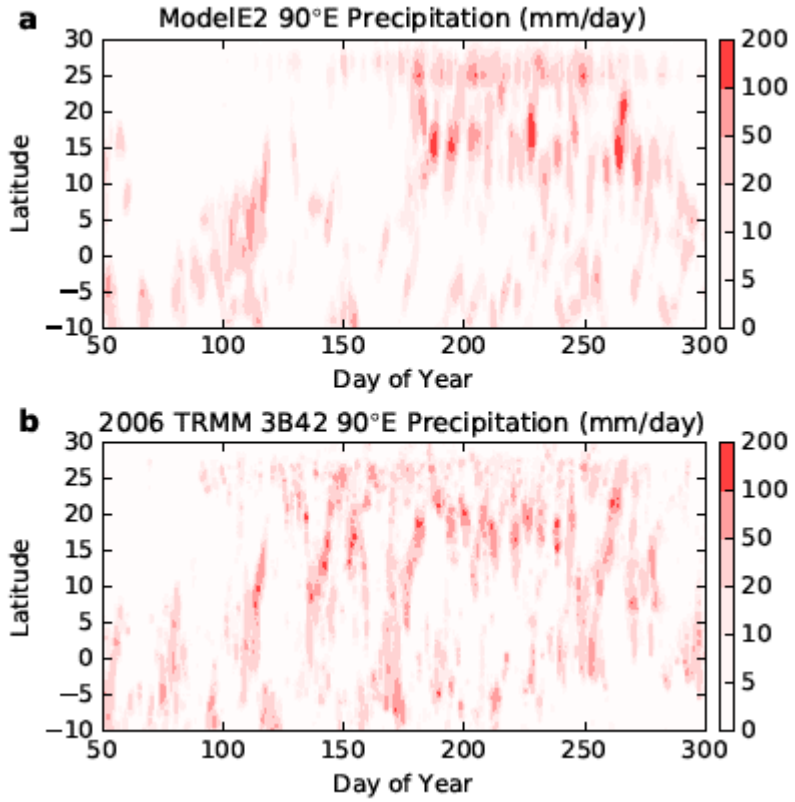

Figure S4. Precipitation (mm day^{-1}) near 90°E (an average between 87.5 and 92.5°E) (a) as simulated by ModelE2 during the first year and (b) retrieved by TRMM during 2006.

Text S3. Identifying Dust Sources that Contribute to the Correlation of Arabian Sea AOD and Central India Precipitation

According to both ModelE2 and the observational analysis of *Vinoj et al.*, [2014], the correlation of weekly averaged precipitation and AOD is positive (and largest) over the Arabian Sea, but negative upwind within the Arabian Peninsula (Figure 1h). This raises the question, at least with regard to ModelE2 where the dust source can be identified, of why there is not a positive correlation of AOD and Indian precipitation along the entire plume trajectory extending from the Arabian Sea to the dust sources within southern Iraq and the Tigris and Euphrates river valleys, where emission is highly correlated with Indian monsoon precipitation (Figure 3). More generally, this raises the question of whether dust sources from another region makes the dominant contribution to AOD over the Arabian Sea.

We believe that the alternating sign of the AOD correlation along the ostensible plume trajectory (parallel to the northwesterly Shamal winds) is the result of reversals in the direction of transport that are rapid compared to the weekly averaging period used to calculate the spatial pattern of correlation [*Vinoj et al.*, 2014]. That is, southern Iraq is indeed the source of Arabian Sea dust in the model, but the negative correlation over the Arabian Peninsula results from aliasing these sub-weekly transport variations when correlating weekly averages.

In general, AOD results from a complicated balance between dust emission upwind, and subsequent transport along with deposition. In our model, emission within the Tigris and Euphrates valleys regresses strongly against monsoon precipitation throughout the entire analysis period of each figure (corresponding to lags between -3 and +3 days relative to Central India precipitation), although emission is slightly larger and more extensive at negative lags. Early in the analysis period (at negative lags), the northwesterly winds near the surface are strongest (Figure 3), and reinforced by the overlying winds near 840 hPa; (Figure 1a). Two days later, the northwesterly surface winds are weaker and the 840 hPa flow has reversed direction, becoming southerly (Fig 1c). A few days after this, the 840 hPa winds are northeasterly or easterly (Figures 1e and f). These variations in wind direction generally correspond to a reduction in AOD along the northwesterly trajectory connecting the Tigris and Euphrates river valleys to the Arabian Sea (Figures 1c, e-g), as dust is deflected from this path, consistent with the negative correlation of weekly averaged AOD over the Arabian Peninsula in Figure 1h (and observed by *Vinoj et al.*, 2014). Thus, the negative correlation of the weekly averages over the Arabian Peninsula and ostensible trajectory of the dust reaching the Arabian Sea result from transport that varies in direction within this averaging period.

The observed negative correlation over the Arabian Peninsula, as analyzed by *Vinoj et al.* [2014], may have an alternative explanation: dust from the Arabian Sea may receive significant contributions from another source. In ModelE2, the Tigris and Euphrates river valley appear to make the leading contribution to Arabian Sea dust, but this result may depend upon the regional distribution of dust sources prescribed in the model.

The Sistan Basin in southeastern Iraq is a potential source of Arabian Sea dust [c.f. *Kaskaoutis et al.,* 2014]. In ModelE2, the winds from this source region are northerly prior to and coincident with precipitation over Central India (Fig 1b-e). A prescription of dust sources that gives greater emphasis to the Sistan Basin would allow a larger contribution to Arabian Sea AOD from this region. We think the source of dust over the Arabian Sea that is correlated with weekly averaged precipitation over Central India is interesting for remaining unsettled.

References:

Gadgil, S. (2003), The Indian monsoon and its variability, *Annual Review of Earth and Planetary Sciences,* 31(1), 429–467, doi: 10.1146/annurev.earth.31.100901.141251.

Huffman, G. J., R. F. Adler, D. T. Bolvin, and G. Gu (2009): Improving the global precipitation record: GPCP Version 2.1, *Geophys. Res. Lett.,* 36, L17808, doi:10.1029/2009GL040000.

Huffman, G. J., R. F. Adler, D. T. Bolvin, E. J. Nelkin, 2010: The TRMM Multi-satellite Precipitation Analysis (TMPA). Chapter 1 in Satellite Rainfall Applications for Surface Hydrology, F. Hossain and M. Gebremichael, Eds. Springer Verlag, ISBN: 978-90-481-2914-0, 3-22.

Kaskaoutis, D., Rashki, A., Houssos, E., Goto, D., and Nastos, P. (2014), Extremely high aerosol loading over Arabian Sea during June 2008: The specific role of the atmospheric dynamics and Sistan dust storms, *Atmos. Environ.,* 94, 374–384.

Kalnay, E., Kanamitsu, M., Kistler, R., Collins, W., Deaven, D., Gandin, L., Iredell, M., Saha, S., White, G., Woollen, J., Zhu, Y., Leetmaa, A., Reynolds, R., Chelliah, M., Ebisuzaki, W., Higgins, W., Janowiak, J., Mo, K. C., Ropelewski, C., Wang, J., Jenne, R., and Joseph, D.: The NCEP/NCAR 40-Year Reanalysis Project, *B. Am. Meteorol. Soc.,* 77, 437–471, doi:10.1175/1520- 0477(1996)077<0437:TNYRP>2.0.CO;2, 1996.

Vinoj, V., P. J. Rasch, H. Wang, J. H. Yoon, P. L. Ma, K. Landu, and B. Singh (2014), Short-term modulation of Indian summer monsoon rainfall by West Asian dust, *Nat. Geosci.,* 7(4), 308–313, doi:10.1038/ngeo2107.